

Influence of superstrong magnetic fields due to strongly electron screening on resonant nuclear reaction $^{23}\text{Mg} (p, \gamma) ^{24}\text{Al}$ in magnetars

Jing-Jing Liu¹, Qiu-He, Peng², Liang-huan, Hao¹, and Dong-Mei, Liu¹

¹ College of Marine Science and Technology, Hainan Tropical Ocean University, Sanya, Hainan 572022, China

² Department of Astronomy, Nanjing University, Nanjing, Jiangsu 210000, China

qhpeng@nju.edu.cn

Received _____; accepted _____

Not to appear in Nonlearned J., 45.

¹Corresponding author: syjjliu68@qzu.edu.cn

ABSTRACT

Basing on the relativistic theory in superstrong magnetic fields (SMFs), we investigate the influence of strong electron screening (SES) on the rates of nuclear reaction $^{23}\text{Mg} (p, \gamma) ^{24}\text{Al}$ by three models of Lai (LD), Fushiki et al. (FGP), and Liu et al. (LJ) on the surface of magnetars. Our results show that the rates can be greatly enhanced by three orders of magnitude due to the influence of SES. The rates in our model are in good agreement with those of LD and FGP at relatively low density environment (e.g. $\rho_7 < 0.01$) for $1 < B_{12} < 10^2$. On the other hand, in relatively high magnetic fields (e.g. $B_{12} > 10^2$), the rates of our model can be 1.58 times and around three orders of magnitude larger than those of FGP and LD, respectively. The significant increase of the rates of our model for $^{23}\text{Mg} (p, \gamma) ^{24}\text{Al}$ implies that more ^{23}Mg will escape from the Ne-Na cycle due to SES in SMFs. As a consequence, the next reaction $^{24}\text{Al} (\beta^+, \nu) ^{24}\text{Mg}$ will produce more ^{24}Mg to participate in the Mg-Al cycle. Thus, it may lead to synthesize a large amount of production of $A \geq 20$ nuclides (e.g. ^{26}Al) on the surface of magnetars. These heavy elements (e.g. ^{26}Al) may be thrown out due to the compact binary mergers of double neutron star (NS-NS) or black hole and neutron star (BH and NS) systems. Our results may help to understand why the ^{26}Al is always overabundance in the interstellar space. Our conclusion may be helpful to the investigation of the nucleosynthesis of some heavy elements, the energy generation rate, and the numerical calculations of magnetars evolution.

Subject headings: dense matter— nuclear reactions, nucleosynthesis, abundances— stars: magnetic fields—stars: interiors

1. Introduction

It is well known that explosive hydrogen burning will take place in high temperature and high hydrogen dense sites in the universe, such as novae, X-ray bursts and supernova. The nucleosynthesis of this burning is called the rapid-proton (rp) process (Wallace et al. 1981). In the stage of stellar explosive burning of hydrogen, a great quantity of proton capture reactions and β^+ -decays (rp-process) will be ignited for those of nuclear mass number $A > 20$. The rp-process might be one of the most important mechanisms for energy production and nucleosynthesis in a variety of astrophysical and pivotal sites with different temperature and density conditions.

According to the stellar evolution theory, for sufficient high temperature in the Ne-Na cycle, the timescale of the proton capture reaction of ^{23}Mg is shorter than that of the β^+ -decay. Therefore, some ^{23}Mg will kindle and escape from the Ne-Na cycle by proton capture. The ^{23}Mg leaks from the Ne-Na cycle into the Mg-Al cycle and results in the synthesis of a large amount of heavy nuclei. Thus the reaction rate of $^{23}\text{Mg} (p, \gamma) ^{24}\text{Al}$ in stellar environment is important and key calculation for synthesis of the heavy nuclei. Due to its significance for nucleosynthesis in astrophysical surroundings, the nuclear reaction rate of $^{23}\text{Mg} (p, \gamma) ^{24}\text{Al}$ has been studied by many previous works. By considering the contribution of a single resonance energy state, Wallace et al. (1981) firstly discussed the reaction rate of $^{23}\text{Mg} (p, \gamma) ^{24}\text{Al}$. Then, considering three resonances and in addition a contribution from the direct capture process, Iliadis et al. (2001) also investigated this nuclear reaction rates. Basing on four resonances and the structure of ^{24}Al , Kubono et al. (1995) reconsidered the rate. Herndl et al. (1998); Visser et al. (2007); Lotay et al. (2008) also carried out an estimation for the rate based on some new experimental information on ^{24}Al excitation energies. Whereas, above of them seem to have overlooked one important influence of electron screening on nuclear reaction.

The strong electron screening (SES) has always been a challenging problem on the stellar weak-interaction rates and thermonuclear reaction rates in pre-supernova stellar evolution and nucleosynthesis. Some pioneering works (Bahcall et al. 2002; Liu 2013, 2014) have been done on stellar weak-interaction rates and thermonuclear reaction rates. In high-density plasma circumstances, the SES has been widely investigated on the basis of various screened Coulomb model, such as Salpeter’s model (Salpeter 1954; Salpeter et al. 1969), Graboske’s model (Graboske et al. 1973), Dewitt’s model (Dewitt et al. 1976). Recently these issues have been discussed by Liolios et al. (2000, 2001), Kravchuk et al. (2014), Liu (2013). However, they neglect the effects of SES on thermonuclear reaction rate in high-density and superstrong magnetic fields (SMFs). How does the SES influence the pre-supernova explosion, nucleosynthesis and thermonuclear reaction in SMFs? What role does the SES play in magnetars? These problems are interesting for us to understand the physical mechanism of SES in dense stars, especially for magnetars.

It is universally accepted that the magnetic fields strength on the surface of some magnetars has the range from 10^{13} to 10^{15} G (Peng et al. 2007; Gao et al. 2013; Lai 2001). The momentum space of the electron gas is changed very asymmetrically by so large SMFs. The electron Fermi energy and nuclear reaction are also affected greatly by SMFs in magnetars. In this paper, according to the relativistic theory in SMFs (Peng et al. 2007; Gao et al. 2013), we carried out an estimation on the SES and electron energy change due to the influence of SMFs. We also discuss how to effects on the thermonuclear reaction by three SES models on the Surface of magnetars.

Our work differs from earlier works (LD and FGP)(Lai 2001; Fushiki et al. 1989) in which we derive new results for the SES theory in an SMFs and the screening rates for nuclear reaction in relativistic strongly magnetic field surrounding basing on the Dirac δ -function and Pauli exclusion principle. We also make detailed comparison among the

results for the nuclear reaction rates of different SES model in SMFs. The main problems, we investigated are how magnetic fields influence the electron Fermi energy and electron screening potential then enters the theory of nuclear reaction rates. We show that this effect can increase nuclear reaction rates by several orders magnitude.

The article is organized as follows. In the next section, we analyse three SES models in SMFs in magnetars. In Section 3 we discuss the effects of SES on the proton capture reaction rate of ^{23}Mg , in which the four resonances contribution will also be considered. The results and discussions will be shown in Section 4. The article is closed with some conclusions in Section 5.

2. The SES in an SMFs

In astrophysical systems, SMFs may have significant influence on the quantum processes. In this Section, we will study three models of the electron screening potential (ESP) in SMFs, i.e., our model (LJ), Lai’s model (LD), and Fushiki et al.’s model (FGP).

2.1. ESP of our model

An SMFs is considered along the z -axis according to relativistic theory in SMFs. And the Dirac equation can be solved exactly. The positive energy levels of an electron in SMFs are given by (Peng et al. 2007; Landau et al. 1977)

$$\frac{\varepsilon_n}{m_e c^2} = \left[\left(\frac{p_z}{m_e c} \right)^2 + 1 + 2 \left(n + \frac{1}{2} + \sigma \right) b \right]^{1/2} = (p_z^2 + \Theta)^{1/2}, \quad (1)$$

where $\Theta = 1 + 2 \left(n + \frac{1}{2} + \sigma \right) b$, $n = 0, 1, 2, 3, \dots$, $b = \frac{B}{B_{\text{cr}}} = 0.02266 B_{12}$, B_{12} is the magnetic fields in units of 10^{12}G , i.e., $B_{12} \equiv B/10^{12}\text{G}$, $B_{\text{cr}} = \frac{m_e^2 c^3}{e \hbar} = 4.414 \times 10^3 \text{G}$ and p_z is the electron momentum along the field, σ is the spin quantum number of an electron, $\sigma = 1/2$,

when $n = 0$, $\sigma = \pm 1/2$, when $n \geq 1$.

In an extremely strong magnetic field ($B \gg B_{cr}$), the Landau column becomes a very long and very narrow cylinder along the magnetic field. How does the quantization of Landau levels change truly by SMFs? It is a very interesting issue for us to discuss. In order to understand the quantization of Landau levels, by introducing the Dirac δ -function $\delta(\frac{p_{\perp}}{m_e c} - [2(n + \sigma + \frac{1}{2})b]^{\frac{1}{2}})$ the eigenvector wave function of the Schrödinger equation will be expanded in an infinite series. When the wave function is limited, by truncating the infinite series we must at firstly give a p_z , then solve the relativistic Schrödinger equation. Finally the maximum Landau level number, n_{max} will be obtained. According to Refs.(Peng et al. 2007; Gao et al. 2013), the electrons degeneracy of the n -th Landau level in a relativistic magnetic field is given by

$$\begin{aligned} \omega_n &= \frac{1}{h^2} g_{n0} \int_0^{2\pi} d\theta \int \delta\left(\frac{p_{\perp}}{m_e c} - [2(n + \sigma + \frac{1}{2})b]^{\frac{1}{2}}\right) p_{\perp} dp_{\perp} \\ &= \frac{2\pi}{h^2} g_{n0} \int \delta\left(\frac{p_{\perp}}{m_e c} - [2(n + \sigma + \frac{1}{2})b]^{\frac{1}{2}}\right) p_{\perp} dp_{\perp} \quad , \end{aligned} \quad (2)$$

where p_{\perp} is the electron momentum perpendicular to the magnetic field, $\theta = \arctan p_y/p_x$, and $g_{n0} = 2 - \delta_{n0}$ is the electron spin degeneracy (when $n = 0$, $g_{00} = 1$; otherwise, $g_{n0} = 2$). According to the Pauli exclusion principle, the electron number density should be equal to its microscopic state density. Thus we have (Peng et al. 2007; Gao et al. 2013)

$$\begin{aligned} N_{phase} = n_e &= 2\pi \frac{(m_e c)^3}{h^3} \int_0^{\frac{E_F(e)}{m_e c^2}} d\left(\frac{p_z}{m_e c}\right) \sum_{n=0}^{n_{max}(p_z, \sigma, b)} \sum g_{n0} \\ &\int_0^{\frac{E_F(e)}{m_e c^2}} \delta\left(\frac{p_{\perp}}{m_e c} - [2(n + \sigma + \frac{1}{2})b]^{\frac{1}{2}}\right) \frac{p_{\perp}}{m_e c} d\left(\frac{p_{\perp}}{m_e c}\right) = N_A \rho Y_e \quad . \end{aligned} \quad (3)$$

According to Equ.(3), the electron chemical potential is determined from the inverting expression for the lepton number density (Peng et al. 2007; Gao et al. 2013, 2012)

$$n_e = \frac{3\pi}{b N_A} \left(\frac{m_e c}{h}\right)^3 \varepsilon_n^4 \int_0^1 \left(1 - \frac{1}{\varepsilon_n^2} - x^2\right) dx - \frac{2\pi \varepsilon_n}{N_A} \left(\frac{m_e c}{h}\right)^3 \sqrt{2b}$$

$$= \frac{\Theta}{2\pi^2\lambda_e^3} \sum_{n=0}^{\infty} g_{n0} \int_0^{\infty} (f_{-e} - f_{+e}) dp_z, \quad (4)$$

where $x = \frac{p_z c}{\varepsilon_n}$, $Y_e = \frac{Z}{A}$ is the electron fraction, N_A is the Avogadro constant, m_e is the electron mass and c is the light speed. $\lambda_e = \frac{h}{m_e c}$ is the Compton wavelength, $f_{-e} = [1 + \exp(\frac{\varepsilon_n - U_F - 1}{kT})]^{-1}$ and $f_{+e} = [1 + \exp(\frac{\varepsilon_n + U_F + 1}{kT})]^{-1}$ are the electron and positron distribution functions respectively, k is the Boltzmann constant, T is the electron temperature and U_F is the electron chemical potential.

Some authors (Lai et al. 1991; Lai 2001; Das et al. 2012) discussed the problem about the electron Fermi energy and Landau level in SMFs. Their results show that the stronger the magnetic field, the smaller the maximum electron Landau level number becomes, as well as electron Fermi energy. According to the theory of quantum mechanics, with increasing of the strength of magnetic fields, the number of electrons of exciting level ($n \geq 1$) will decrease. On the other hand, when $B \gg B_{cr}$, then $n_{max} = 1$ or 2 , and a great deal of electrons will occupy in the ground level. Accordingly it is undoubted that the momentum p_z and p_{\perp} will decrease. However, according to the Dirac Delta-function $\delta(\frac{p_{\perp}}{m_e c} - [2(n + \sigma + \frac{1}{2})b]^{\frac{1}{2}})$, one can find that, when we give a certain Landau level number n , both the momentum $p_{\perp}(n) \sim m_e c [2(n + \sigma + \frac{1}{2})b]^{\frac{1}{2}}$ and the magnetic energy $E_B(n) \sim p_{\perp}(n)c \sim m_e c^2 [2(n + \sigma + \frac{1}{2})b]^{\frac{1}{2}}$ will increase with increasing the strength of magnetic fields, which lead to more electrons contribute to $p_{\perp}(n)$ and $E_B(n)$. Therefore, a good many electrons will occupy at a certain Landau level as the strength of magnetic fields increase. It is the same as $\Delta p_{\perp}(n, n+1)$, which is the difference of p_{\perp} between two adjacent landau levels at a certain Landau level n . On the contrary, $\Delta p_{\perp}(n, n+1)$ decreases with increasing n when the strength of magnetic fields is certain.

Based on the above discussions and Equ.(4), the Fermi energy of the electron is given

by (Gao et al. 2013)

$$\begin{aligned} E_F &= U_e = 43.44 \times 10^3 \left(\frac{B}{B_{\text{cr}}}\right)^{1/4} \left(\frac{\rho Y_e}{\rho_0 \times 0.0535}\right)^{1/4} \\ &= 43.44 \times 10^3 \left(\frac{B}{B_{\text{cr}}}\right)^{1/4} \left(\frac{n_e}{0.0535 \times \rho_0 N_A}\right)^{1/4} \text{keV}, \end{aligned} \quad (5)$$

where $\rho_0 = 2.8 \times 10^4 \text{g/cm}^3$ is standard nuclear density.

In order to evaluate the Thomas-Fermi screening wave-number $K_{\text{TF}}^{\text{LJ}}$, we defined a parameter $D^{\text{LJ}}(U_e)$ and according to Equ.(5), we have $n_e = \frac{0.0535 \rho_0 N_A}{b} \left(\frac{U_e}{43.44 \times 10^4}\right)^4$ and

$$D^{\text{LJ}}(U_e) = \frac{\partial n_e}{\partial U_e} = \frac{\partial}{\partial U_e} \left(\frac{0.0535 \rho_0 N_A}{b} \left(\frac{U_e}{43.44 \times 10^4}\right)^4\right) = 1.5057 \times 10^5 (n_e)^{3/4} b^{-1/4}. \quad (6)$$

According to Equ.(6), the Thomas-Fermi screening wave-number $K_{\text{TF}}^{\text{LJ}}$ is given by (Ashcroft et al. 1976)

$$(K_{\text{TF}}^{\text{LJ}})^2 = 4\pi e^2 D^{\text{LJ}}(U_e) = 4\pi e^2 \frac{\partial n_e}{\partial U_e} = 1.8921 \times 10^6 e^2 (n_e)^{3/4} b^{-1/4}. \quad (7)$$

The binding energy of the magnetized condensed matter at zero pressure can be estimated using the uniform electron gas model (Kadomtsev 1970). When the magnetic field is enough strong, the electrons only occupy the ground Landau level. The energy per cell can be written as

$$E_{\text{total}} = E_k + E_{\text{latt}} = \frac{3\pi^2 e^2 z_j^3}{8b_1^2 r_i^6} + \frac{9e^2 z_j^{5/3}}{10r_e}, \quad (8)$$

where the first term is the kinetic energy and the second term is the lattice energy.

$r_i = z^{1/3} r_e a_0$ is the Wigner-Seitz cell radius, $a_0 = 0.529 \times 10^{-8} \text{cm}$ is the Bohr radius,

and $r_e = \left(\frac{3}{4\pi n_e}\right)^{1/3}$ is the mean electron spacing. z_j is the charge number of the species j .

$b_1 = \frac{B}{B_0} = 425.4 B_{12} = 1.9773 \times 10^4 b$ and $B_0 = \frac{m_e^2 c e^3}{\hbar^3} = 2.3505 \times 10^{-9} \text{G}$. For the zero-pressure condensed matter, we require $\frac{dE_{\text{total}}}{dr_i} = 0$, so we have $r_i = r_{i0} = 0.0371 z_j^{1/5} b^{-2/5} a_0$.

Basing on above discussion, the energy correction per cell due to non-uniformity can be calculated by using linear response theory, which gives by (Lattimer et al. 1985)

$$E_{\text{TF}}^{\text{LJ}}(r_i, z_j) = -\frac{18}{175} (K_{\text{TF}}^{\text{LJ}} r_i)^2 \frac{(z_j e)^2}{r_i} = -\frac{2.0730 e^4 (n_e)^{3/4} (\rho_0 N_A)^{1/4} z_j^{11/5}}{b^{13/20}}. \quad (9)$$

For the relativistic electron, the influence from exchange free energy has been discussed by Stolzmann et al. (1996); Yakovlev et al. (1989). Their works showed that the correlation correction is very small. Therefore, in this paper we have neglected the correction of Coulomb exchange free energy interaction in the electron gas model. By taking into consideration of the Coulomb energy and Thomas-Fermi correction due to non-uniformity of the electron gas, the energy per cell should be corrected as

$$E_s^{\text{LJ}}(r_i, z_j) = E_k(r_i, z_j) - U_{\text{coul}}(r_i, z_j) - E_{\text{TF}}^{\text{LJ}}(r_i, z_j). \quad (10)$$

For two interaction nuclides, the energy required to bring two nuclei with nuclear charge numbers z_1 and z_2 so close together that they essentially coincide differs from the bare Coulomb energy by an amount which in the Wigner-Seitz approximation is

$$U_{\text{sc}} = E_s(r_i, z_{12}) - E_s(r_i, z_1) - E_s(r_i, z_2), \quad (11)$$

where $z_{12} = z_1 + z_2$. If the electron distribution is rigid, the contribution to from E_s the bulk electron energy cancel in expression (10), and the screening potential is simply

$$\begin{aligned} U_{\text{sc}} &= E_{\text{coul}}(r_i, z_{12}) - E_{\text{coul}}(r_i, z_1) - E_{\text{coul}}(r_i, z_2) \\ &= 6.5984 \times 10^4 b^{2/5} (z_{12}^{9/5} - z_1^{9/5} - z_2^{9/5}), \text{ MeV} \end{aligned} \quad (12)$$

when the electron density is assumed to be uniform, the screening potential is independent of the magnetic field. However, the electrons are not rigid and they respond to the ionic potential. Their compressibility depends on the magnetic field, and this leads in turn to a field dependence of the screening potential. Note that expression (10) for the energy contains contributions not only from the Coulomb interaction, but also ones from the compressibility energy of the electron in the non-uniform state.

From expression (9), the change of the screening potential due to the compressibility of the electrons for the zero-pressure magnetized condensed matter can obtained as

$$\delta E_{\text{TF}}^{\text{LJ}} = -\frac{18}{175} (K_{\text{TF}}^{\text{LJ}} r_i)^2 \frac{e^2 (z_{12}^2 - z_1^2 - z_2^2)}{r_i}$$

$$= -\frac{2.0730e^4 n_e^{3/4} (z_{12}^{11/5} - z_1^{11/5} - z_2^{11/5})}{b^{13/20}}. \quad (13)$$

In accordance with above discussions, the screening potential is sum of the screening potential with a uniformity distribution and a corrected screening potential with a non-uniformity distribution. The screening potential in SMFs is given by

$$U_{sc}^{LJ} = U_{sc} + \delta E_{TF}^{LJ}. \quad (14)$$

2.2. ESP of LD's model

Lai (2001) and Lai et al. (1991) discussed the states equation in neutron stars and electron energy in SMFs. In SMFs the number density n_e of electrons is related to the chemical potential U_e by

$$n_e = \frac{1}{(2\pi\hat{\rho})^2 \hbar} \sum_0^\infty g_{n0} \int_{-\infty}^{+\infty} f dp_z = \frac{1}{(2\pi\hat{\rho})^2 \hbar} \sum_0^\infty g_{n0} \int_{-\infty}^{+\infty} [1 + \exp(\frac{E - U_e}{kT})]^{-1} dp_z, \quad (15)$$

$$\hat{\rho} = (\frac{\hbar c}{eB})^{1/2} = 2.5656 \times 10^{-10} B_{12}^{1/2} \text{ cm}, \quad (16)$$

where $E = [c^2 p_z^2 + m_e c^4 (1 + nb)]^{1/2}$ is free electron energy, g_n is the spin degeneracy of the Landau level, $g_{00} = 1$ and $g_{n0} = 2$ for $n \geq 1$, and the Fermi-Dirac distribution is given by

$$f = [1 + \exp(\frac{E - U_e}{kT})]^{-1}. \quad (17)$$

The electron Fermi energy, which includes the electron rest mass $E_F = U_e(kT = 0) - m_e c^2$ is given from

$$n_e = \frac{1}{2\pi^{3/2} \lambda_{Te} \hat{\rho}^2} \sum_{(n=0)}^\infty g_n I_{-1/2}(\frac{U_e - n\hbar\omega_{ce}}{kT}), \quad (18)$$

where the thermal wavelength of the electron is $\lambda_{Te} = (\frac{2\pi\hbar^2}{m_e kT})^{1/2}$, and the Fermi integral is written as

$$I_n(y) = \int_0^\infty \frac{x^n}{\exp(x - y) + 1} dx. \quad (19)$$

The binding energy of the magnetized condensed matter at zero pressure can be estimated using the uniform electron gas model. Under the condition of super-strong magnetic field, the Fermi energy U_F is less than the cyclotron energy $\hbar\omega_{ce}$, the electrons only occupy the ground Landau level. According to the theory in SMFs of Refs.(Lai 2001), the Thomas-Fermi screening wave-number is given by

$$(K_{\text{TF}}^{\text{LD}})^2 = 4\pi e^2 D^{\text{LD}}(\varepsilon_F) = 4\pi e^2 \frac{\partial n_e}{\partial \varepsilon_F} = 4\pi e^2 \frac{\partial n_e}{\partial U_F}, \quad (20)$$

where $\frac{\partial n_e}{\partial \varepsilon_F}$ is the density of states per unit volume at the Fermi surface. $\varepsilon_F = \frac{P_F^2}{2m_e}$. Due to $n_e = \frac{2eB}{h^2 c} P_F$, so we have

$$D^{\text{LD}} = \frac{\partial n_e}{\partial \varepsilon_F} = \frac{n_e}{2\varepsilon_F} = \left(\frac{m_e}{n_e}\right) \left(\frac{2eB}{h^2 c}\right)^2 = \frac{3.79 \times 10^6 b^2 r_e^3}{e^2}. \quad (21)$$

The Thomas-Fermi screening wavenumber will be given by

$$K_{\text{TF}}^{\text{LD}} = \left(\frac{4}{3\pi^2}\right)^{1/2} b_1 r_e^{3/2} = 6.901 \times 10^3 b r_e^{3/2}. \quad (22)$$

Using linear response theory, the energy correction (in atomic units) per cell due to non-uniformity can be calculated and gives by (Lai 2001)

$$E_{\text{TF}}^{\text{LD}}(r_i, z_j) = -\frac{18}{175} (K_{\text{TF}}^{\text{LD}} r_i)^2 \frac{e^2 z_j^2}{r_i} = -0.0139 b_1^2 r_i^4 z_j. \quad (23)$$

The uniform electron gas model can be improved by taking into consideration of the Coulomb energy and Thomas-Fermi correction due to non-uniformity of the electron gas. When the electron density is assumed to be uniform, the screening potential is independent of the magnetic field. The change of the screening potential due to the compressibility of the electrons for the zero-pressure magnetized condensed matter can obtained

$$\delta E_{\text{TF}}^{\text{LD}} = -2.5236 \times 10^{-4} b^{2/5} (z_{12}^{9/5} - z_1^{9/5} - z_2^{9/5}). \quad (24)$$

When we summed of the screening potential with a uniformity distribution and a corrected screening potential with a non-uniformity distribution, the screening potential in SMFs is given by

$$U_s^{\text{LD}} = U_{\text{sc}} + \delta E_{\text{TF}}^{\text{LD}}. \quad (25)$$

2.3. ESP of FGP's model

The rate of nuclear reaction in high density matter is affected by the fact that the clouds of the electrons surrounding nuclei alter the interactions among nuclei. The influence of SES in SMF on nuclear reaction was also detailed discussed by Fushiki et al. (1989) (hereafter FGP). The electron Coulomb energy by an amount which in the Wigner-Seitz approximation in SMF was given by

$$U_{\text{sc}}^{\text{FGP}} = E_{\text{atm}}(r_i, z_{12}) - E_{\text{atm}}(r_i, z_1) - E_{\text{atm}}(r_i, z_2), \quad (26)$$

where $E_{\text{atm}}(r_i, z_j)$ is the total energy of Wigner-Seitz cell. If the electron distribution is rigid, the contribution to $E_{\text{atm}}(r_i, z_j)$ from the bulk electron energy cancel, the electron screening potential at high density can be expressed as

$$U_{\text{sc}}^{\text{FGP}} = E_{\text{latt}}(r_i, z_{12}) - E_{\text{latt}}(r_i, z_1) - E_{\text{latt}}(r_i, z_2), \quad (27)$$

where $E_{\text{latt}}(r_i, z_j)$ is the electrostatic energy of Wigner-Seitz cell and $E_{\text{atm}}(r_i, z_j) = \frac{-0.9z_j^{5/3}e^2}{r_e}$. Due to the influence of the compressibility of the electron, the change in the screening potential is given by (Fushiki et al. 1989)

$$\begin{aligned} \delta U_s^{\text{FGP}} &= -\frac{54}{175} \left(\frac{e^2}{r_e}\right) \frac{1}{n_e} \frac{\partial n_e}{\partial U_e} [(z_{12})^{7/3} - (z_1)^{7/3} - (z_2)^{7/3}] \\ &= -\frac{54}{175} \left(\frac{e^2}{r_e}\right) \frac{1}{n_e} D^{\text{FGP}} [(z_{12})^{7/3} - (z_1)^{7/3} - (z_2)^{7/3}], \end{aligned} \quad (28)$$

where

$$D^{\text{FGP}} = 823.1481 \frac{r_e n_e}{e^2} \left(\frac{\bar{A}}{z}\right)^{4/3} \rho^{-4/3} B_{12}^2. \quad (29)$$

The Thomas-Fermi screening wavenumber will be given by

$$(K_{\text{TF}}^{\text{FGP}})^2 = 1.0344 \times 10^4 r_e n_e \left(\frac{\bar{A}}{z}\right)^{4/3} \rho^{-4/3} B_{12}^2. \quad (30)$$

According to the theory of Ref. (Fushiki et al. 1989), the corresponding result for the changes in the screening potential in an SMFs is

$$\begin{aligned} \delta U_s^{\text{FGP}} &= -0.254 \left(\frac{\bar{A}}{z}\right)^{4/3} \rho^{-4/3} B_{12}^2 [(z_{12})^{7/3} - (z_1)^{7/3} - (z_2)^{7/3}] \\ &= -494.668 \left(\frac{\bar{A}}{z}\right)^{4/3} \rho^{-4/3} b^2 [(z_{12})^{7/3} - (z_1)^{7/3} - (z_2)^{7/3}] \text{MeV}, \end{aligned} \quad (31)$$

where $\left(\frac{\bar{A}}{z}\right)$ is the average of $\frac{A}{z}$ ratio, which corresponding to the mean molecular weigh per electron. Thus the electron screening potential in SMFs of FGP's model is given by

$$\begin{aligned} U_s^{\text{FGP}} &= U_{\text{sc}} + \delta E_{\text{TF}}^{\text{FGP}} \\ &= U_{\text{sc}} + \delta U_s^{\text{FGP}}. \end{aligned} \quad (32)$$

3. The resonant reaction process and rates

3.1. The calculation of resonant reaction rates with and without SES

The reaction rates are summed of contribution from the resonant reaction and non-resonant reaction. In the case of a narrow resonance, the resonant cross section σ_r is approximated by a Breit-Wigner expression (Fowler et al. 1967)

$$\sigma_r(E) = \frac{\pi\omega}{\kappa^2} \frac{\Lambda_i(E)\Lambda_f(E)}{(E - E_r)^2 + \frac{\Lambda_{\text{total}}^2(E)}{4}}, \quad (33)$$

where κ is the wave number, the entrance and exit channel partial widths are $\Lambda_i(E)$ and $\Lambda_f(E)$, respectively. $\Lambda_{\text{total}}(E)$ is the total width, and the statistical factor, ω is given by

$$\omega = (1 + \delta_{12}) \frac{2J + 1}{(2J_1 + 1)(2J_2 + 1)}, \quad (34)$$

where the spins of the interacting nuclei and the resonance are J_1 , and J_2 , respectively. δ_{12} is the Kronecker symbol.

The partial widths is depended on the energy, and can be written by(Lane et al. 1958)

$$\Lambda_{i,f} = 2\vartheta_{i,f}^2 \psi_l(E, a) = \Lambda_{i,f} \frac{\psi_l(E, a)}{\psi_l(E_f, a)}. \quad (35)$$

The penetration factor ψ_l is associated with l and a , which are the relative angular momentum and the channel radius, respectively. a is written as $a = 1.4(A_1^{1/3} + A_2^{1/3})$ fm. $\Lambda_{i,f}$ is the partial energy widths at the resonance process. E_r and $\vartheta_{i,f}^2$ is the reduced widths and given by

$$\vartheta_{i,f}^2 = 0.01\vartheta_w^2 = \frac{0.03\hbar^2}{2Aa^2}. \quad (36)$$

Based on the above, in the phases of explosive stellar burning, the narrow resonance reaction rates without SES is determined by (Schatz et al. 1998; Herndl et al. 1998)

$$\lambda_r^0 = N_A \langle \sigma v \rangle_r = 1.54 \times 10^{11} (AT_9)^{-3/2} \sum_i \omega \gamma_i \exp(-11.605 E_{r_i}/T_9) \text{cm}^3 \text{mol}^{-1} \text{s}^{-1}, \quad (37)$$

where N_A is Avogadro's constant, A is the reduced mass of the two collision partners, E_{r_i} is the resonance energies and T_9 is the temperature in unit of 10^9 K. The $\omega \gamma_i$ is the strength of the resonance in MeV and given by

$$\omega \gamma_i = (1 + \delta_{12}) \frac{2J + 1}{(2J_1 + 1)(2J_2 + 1)} \frac{\Lambda_i \Lambda_f}{\Lambda_{\text{total}}}. \quad (38)$$

On the other hand, due to SES the reaction rates of narrow resonance is given by

$$\begin{aligned} \lambda_r^s &= F_r N_A \langle \sigma v \rangle_{r'} = 1.54 \times 10^{11} (AT_9)^{-3/2} \sum_i \omega \gamma_i \exp(-11.605 E'_{r_i}/T_9) \\ &= 1.54 \times 10^{11} F_r (AT_9)^{-3/2} \sum_i \omega \gamma_i \exp(-11.605 E_{r_i}/T_9) \text{cm}^3 \text{mol}^{-1} \text{s}^{-1}, \end{aligned} \quad (39)$$

where F_r is the screening enhancement factor (hereafter SEF). The values of E'_{r_i} should be measured by experiment, but it is too hard to provide sufficient data. In general and approximate analysis, we have $E'_{r_i} = E_{r_i} - U_0 = E_{r_i} - U_s$.

3.2. The screening model of resonant reaction rates in the case without SMFs

3.2.1. Dewitt's model

Dewitt et al. (1976) discussed the problem of thermonuclear ion-electron screening at some densities. Basing on a statistical mechanical theory for the screening function, the influence of the electron screening on the nuclear reaction process also was investigated for all cases of astrophysical interest in their paper. And the strong electron screening potential function is given by (Dewitt et al. 1976)

$$H_{12}^{\text{sc}} = \frac{e^2}{r_e kT} \{0.9(\bar{z})^{1/3}(z_{12}^{5/3} - z_1^{5/3} - z_2^{5/3}) + c_1(\bar{z})^{2/3}(z_{12}^{4/3} - z_1^{4/3} - z_2^{4/3})\} + [c_2(\bar{z})^{-2/3}(z_{12}^{2/3} - z_1^{2/3} - z_2^{2/3})], \quad (40)$$

where $c_1 = 0.2843$ and $c_2 = 0.4600$, and the \bar{z} , the average charge of ionic, is given by

$$\bar{z} = \sum_i z_i f_i = \sum_i z_i \frac{n_i}{n_1}, \quad (41)$$

where n_i and n_1 are the ion densities of nuclear species i and of the total system, respectively.

The screening enhancement factor (hereafter SEF) can be rewritten as

$$F_r^0(Dew) = \exp(H_{12}^{\text{sc}}). \quad (42)$$

3.2.2. Liolios's model

At astrophysical energies the electron-screening acceleration of laboratory fusion reactions always play a key roles and is an interesting problem of great importance to astrophysics. Basing on a mean-field model, Liolios et al. (2000) studied the screened nuclear reactions at astrophysical energies. The electron screening potential in Liolios's screened Coulomb model is given by (Liolios et al. 2000)

$$U_0^{\text{Lios}} = \frac{15}{8} \frac{z_1 z_2 e^2}{\Xi}, \quad (43)$$

$$\Xi = \left(\frac{15}{8\pi z_i^2}\right)^{1/3} a_0 = 0.8853 a_0 (z_1^{2/3} + z_2^{2/3})^{1/2}. \quad (44)$$

We introduce a screening enhancement factor for considering the screening effects. The SEF for the resonant reaction can be expressed as

$$F_r^0(Lios) = \exp\left(\frac{11.605 U_0^{Lios}}{T_9}\right). \quad (45)$$

3.3. The screening model of resonant reaction rates in SMFs

It is widely known that nuclear reaction rates at low energies play a key role in energy generation in stars and the stellar nucleosynthesis. The bare reaction rates are modified in stars by the screening effects of free and bound electrons. The knowledge of the bare nuclear reaction rates at low energies is important not only for the understanding of various astrophysical nuclear problems, but also for assessing the effects of host material in low energy nuclear fusion reactions in matter.

According to some researches and observation data, anomalous X-ray pulsars (AXPs) and soft gamma-ray repeaters (SGRs) are a class of strongly magnetized neutron stars. These neutron stars are named magnetars. Some magnetars may have strong magnetic fields and the strength can be the rang from 10^{14} G to 10^{15} G (Peng et al. 2007; Lai 2001). The Fermi energy of the electron gas may go up to 10 Mev and quantum effects of electron gas will be very obvious and sensitive in SMFs. As we all know, the positive energy levels must be obeyed quanta law due to the electron moves along the z-axis according to Landau's model. The distribution of the electron in the momentum space will be strongly changed by the SMFs. The electron screening will play a key role in this process. It can strongly affect the electron transformation and nuclear reaction rates. In this paper, we will discuss the screening potential in the strong screening limit. The dimensionless parameter (Γ), which determines whether or not correlations between two species of nuclei (z_1, z_2) are

important, is given by

$$\Gamma = \frac{z_1 z_2 e^2}{(z_1^{1/3} + z_2^{1/3}) r_e k T}. \quad (46)$$

Under the conditions of $\Gamma \gg 1$, the nuclear reaction rates will be influence appreciably by SES. According to the above three theoretical SES model (LD, FGP, LJ) in SMFs, the three enhancement factors for resonant reaction process in SMFs can be expressed as follows:

$$F_r^B(LD) = \exp\left(\frac{11.605 U_s^{LD}}{T_9}\right), \quad (47)$$

$$F_r^B(FGP) = \exp\left(\frac{11.605 U_s^{FGP}}{T_9}\right), \quad (48)$$

$$F_r^B(LJ) = \exp\left(\frac{11.605 U_s^{LJ}}{T_9}\right). \quad (49)$$

In order to compare the resonant nuclear rates for some different model under different conditions, we define factors q_j and C_i as follows:

$$q_j = \frac{\lambda_r^{scB}(LJ)}{\lambda_{rj}^{scB}} (j = 1, 2), \quad (50)$$

$$C_i = \frac{\lambda_{ri}^{scB} - \lambda_r^0}{\lambda_r^0} (i = 1, 2, 3), \quad (51)$$

where $\lambda_{rj}^{scB} (j = 1, 2)$ is the rates for LD's and FGP's model in Equ.(50), respectively. In Equ.(51), λ_r^0 is the resonant reaction rates in the case without SES and $\lambda_{ri}^{scB} (i = 1, 2, 3)$ is the rates for models of LD, FGP and LJ in the case with SES and SMFs, respectively.

4. Numerical results

4.1. Analysis of the results on SEF

The strong magnetic fields modify significantly the properties of the matter and always play a critical role in astronomical conditions. In his paper, our main aim is to consider

the problem of SES in SMFs, as well as the Landau energy level, and the electron Fermi energy. According to the relativistic theory in SMFs, we carried out an estimation of the influence on the energy change due to non-uniformity of the electron gas in SMFs. We build a SES model (i.e. LJ’s model) and analysis in detail the influence of SMFs on SES. Figure 1 presents the variations of ESP as a function of B_{12} . The SMF has only a slight influence on ESP when $B_{12} > 10^3$ and $\rho_7 < 1$. But the ESP increases greatly when $0 < B_{12} < 2 \times 10^3$ and $\rho_7 < 1$. Numerical results in our model show that the maximum value of ESP will reach 0.1 MeV.

Some authors have carried out some theoretical researches about the influence on stellar matter by SMFs. Lai (2001) discussed the properties of the matter of the neutron star and given a general review article that covers the broad subject of matter in SMFs. According to Laidong’s theory of SES in SMFs, we analysis the SES model (hereafter LD’s model), which is discussed in Section 2.2 and 3.3. **Figure 2** presents the ESP of LD’s model as a function of B_{12} . The results show that the ESP increases rapidly when $0 < B_{12} < 10$. The ESP reaches the maximum value of 0.008442 MeV at $B_{12} = 80$ according to our calculations. Then the ESP will decrease with increasing of SMFs.

The surface structure of neutron stars with high magnetic fields also was in detail discussed by Fushiki et al. (1989). Based on the Thomas-Fermi and Thomas-Fermi-Dirac approximations, they analyzed the equation of electron state, the electron Fermi energy in Landau level, and SES problem in SMFs. The results show that, as a consequence of the field dependence of the screening potential, magnetic fields can significantly increase nuclear reaction rates (Fushiki et al. 1989). According to electron screening model (hereafter FGP’s model) in SMFs, Figure 2 shows the ESP as a function of B_{12} under some typical astrophysical conditions. The influence of SMFs on ESP is very obvious for relatively low density (e.g. $\rho_7 = 0.01, 0.1$). The ESP increases greatly when $B_{12} < 10^3$ and gets to the

maximum value of 0.0188 MeV at $B_{12} = 580.7$ and $\rho_7 = 0.1$. On the other hand, the ESP decreases around two orders of magnitude when $10^3 < B_{12} < 2 \times 10^3$ at $\rho_7 = 0.1$.

The influence of SES in SMFs on nuclear reaction is mainly reflected by the SEF. We discuss the influence of SES on SEF by three models (LD, FGP, LJ) from **Figure 3 to Figure 4**. One can find that the SEF of LD’s model is a sensitive parameter to SMFs and temperature in Figure 4. The maximum value of SEF is about 1.632 for $B_{12} = 78.17$ and $T_9 = 0.2$. But for $B_{12} > 219.3$ the SEF is less than 1.001.

Figure 4 also presents the SEF as function of B_{12} of FGP’s and LJ’s model. One can see that shifty trend of SEF of FGP’s model is in good agreement with those of LD at low density (e.g. $\rho_7 = 0.01$). The maximum value of SEF of FGP’s model is about 1.66 for $B_{12} = 84.18$ and $\rho_7 = 0.01$. On the contrary, the SEF increases greatly with increasing of B_{12} at relatively high density (e.g. $\rho_7 = 1$), then gets to the maximum value of 5.166 at $T_9 = 0.2$. The information of SEF of LJ’s model also shows that the SEF increases with increasing of B_{12} . The maximum value will reach 5.056 for $B_{12} = 1000$, $T_9 = 0.2$ and $\rho_7 = 0.01$.

In **Figure 5**, we show some comparisons for some typical astronomical condition of the resonant SEF among the models of LJ, LD, and FGP in SMFs. According to our calculations, we find the results of LD’s model are well agreement with those of FGP for relatively low density (e.g. $\rho_7 \leq 0.01$). Nevertheless, the SEF of our model decreases very placid with the increasing of B_{12} and T_9 to compare with those of LD’s and FGP’s.

The SES problem always plays important roles in stellar evolution process. Basing on a statistical mechanical theory for the screening function, Dewitt et al. (1976) investigated the influence of the electron screening on nuclear reaction. Based on a mean-field model, Liolios et al. (2000) also in detail studied the effect about screened nuclear reactions. However, their works neglect the influence of SES in SMFs. We compare the SEF of the

two SES models (Dewitt’s, and Liolios’ model) with those of three SES models (LD, FGP, and LJ). One can conclude that the SEF of Dewitt’s model is larger than those of other three SES models for $B_{12} < 140$, $\rho_7 = 0.01$ and $T_9 < 0.17$ in **Figure 6**. However, when $T_9 < 0.18$, $\rho_7 = 0.01$, the results of our model (LJ) are larger than those of Dewitt and Liolios. In relatively high density (e.g. $\rho_7 = 0.1$), the SEF of LD’s, FGP’s and LJ’s models will decrease due to SMFs and is lower than those of Dew’s model. The results obtained by Dewitt et al. (1976) amounts to an overestimation of the screening effect because of their neglect of spatial dependence of the screening function.

Table 1 shows some information about the five SEF at some astronomical conditions. We can find the results of LD, FGP, and LJ are always lower than those of Liolios and Dewitt due to the influence of SMFs. And the SEF of our model decreases very greatly with increasing of density and temperature when $B_{12} = 10^3$. It is because that the ESP increases very quickly with increasing of SMFs. The higher the ESP, the larger the influence on SES becomes. On the contrary, the SEF of LD will decrease with increasing of magnetic fields due to the ESP is reduced by SMFs. The SEF of FGP’s model will get to the maximum of 1.929 when $B_{12} = 10^3$, $\rho_7 = 1$, $T_9 = 0.5$ and then decreases slowly as increasing of density and temperature.

The Thomas-Fermi screening wave-number K_{TF} is a very key parameter, which is strongly depend on electron number density and ESP. In consequence the electron number density and ESP will play important roles when we discuss the problem of SES in SMFs. Basing on the uniform electron gas model and linear response theory, Lai (2001) discussed electron energy (per cell) corrections due to non-uniformity in SMFs. The LD’s model is valid only for $K_{TF}r_i \ll 1$ at lower densities and investigated the non-uniformity effect only through detailed electronic (band) structure calculations. Lai et al. (1991), Das et al. (2012) also in detail analyzed the electron Fermi energy and electron number density in SMFs

basing on the theory of Canuto et al. (1968, 1971); Kubo. (1965), and Pathria (2003). We know the microscopic state number $dx dy dz dp_x dp_y dp_z$ can be given by $dx dy dz dp_x dp_y dp_z / h^3$ in a 6-dimension phase-space according to statistical physics. The number of states occupied by completely degenerate relativistic electrons per volume is calculated by (Canuto et al. 1968, 1971)

$$\begin{aligned} N_{phase} &= \sum_{p_x} \sum_{p_y} \sum_{p_z} = \frac{1}{h^3} \int_{-\infty}^{\infty} \int_{-\infty}^{\infty} \int_{-\infty}^{\infty} dp_x dp_y dp_z \\ &= \frac{1}{h^3} \int_0^{p_F} dp_z \int_0^{\infty} p_{\perp} dp_{\perp} \int_0^{2\pi} d\theta = \frac{\pi p_F}{h^3} \int_0^{\infty} dp_{\perp}^2, \end{aligned} \quad (52)$$

where $\theta = \tan^{-1} p_y / p_x$, $p_{\perp}^2 \rightarrow m^2 c^4 \frac{B}{B_{cr}} 2n$, So, $\int_0^{\infty} dp_{\perp}^2 \rightarrow \sum_{n=0}^{\infty} \omega_n$, and the ω_n is the degeneracy of the n -th electron Landau level in relativistic magnetic field, and can be calculated by (Canuto et al. 1971; Kubo. 1965; Pathria 2003)

$$\begin{aligned} \omega_n &= \frac{1}{h^2} \int_0^{2\pi} d\phi \int_{k_1 < p_{\perp}^2 < k_2} p_{\perp} dp_{\perp} \\ &= \frac{2\pi (k_2 - k_1)}{h^2} = \frac{1}{2\pi} \left(\frac{\hbar}{m_e c} \right)^{-2} \frac{B}{B_{cr}} = \frac{b}{2\pi} \left(\frac{\hbar}{m_e c} \right)^{-2}, \end{aligned} \quad (53)$$

where $k_1 = 2nm_e^2 c^2 \frac{B}{B_{cr}} = 2nbm_e^2 c^2$, and $k_2 = 2(n+1)bm_e^2 c^2$. According to these theory in SMFs, and by using the solution of the non-relativistic electron cyclotron motion, $\hbar\omega_B = 2\mu_e B$, Lai et al. (1991); Lai (2001), and Das et al. (2012) analyzed the electron Fermi energy and electron number density in SMFs. Their expression for the degeneracy electron of the n -th Landau level in a relativistic magnetic field is completely took the place of that for the corresponding non-relativistic case. Therefore, Lai et al. (1991); Lai (2001) obtained that the electron Fermi energy $E_F(e)$, can be decreased with increasing of magnetic field strength in superstrong magnetic field environment (i.e. $E_F(e) = U_F \propto 2.70 B_{12}^{-2} k(Y_e \rho)^2$). Basing on above theory, we study the ESP and the SES model (LD's model). The results show that the ESP will decrease with increasing of magnetic fields due to the diminution of electron chemical potential. Maybe it lead to a different inevitable influence on SES in SMFs.

On the other hand, the electron chemical potential is a pivotal parameter, which is closely related to the electron number density and exchange energy. Basing on Thomas-Fermi-Dirac approximation, it is given by (Fushiki et al. 1989)

$$U_F = U_e = \frac{\partial w_{\text{ex}}}{\partial n_e} = \frac{r_{\text{cyc}}}{\pi a_0} \hbar \omega_0 n I(n), \quad (54)$$

where w_{ex} is the exchange energy and $I(n)$ can be find in Ref. (Fushiki et al. 1989). Using the linear response theory, Fushiki et al. (1989) discussed the exchange energy and electron chemical potential in the lowest Landau level for non-uniformity electron gas due to SMFs. They analyzed the SES problem in SMFs and their results shown that due to SMFs only the lowest Landau level is occupied on the condition of $r_e > (3\pi/8)^{1/3} r_{\text{cyc}}$ or equivalently $\rho < 7.04 \times 10^3 B_{12}^{3/2} (\text{A/z}) \text{g/cm}^3$ by electrons. The cyclotron radius in the lowest Landau level orbital is give by $r_{\text{cyc}} = (2\hbar c/eB)^{1/2} \simeq 3.36 \times 10^{-10} B_{12}^{-1/2}$. But for the free electron gas FGP used the expression of $\frac{\partial n_e}{\partial U_F} n_e = (3/2) \frac{n_e}{U_F}$ when they deal with $\frac{\partial n_e}{\partial U_F}$. In FGP's model, they think at high density the exchange correction is very small, thus they neglect the exchange correction to $\frac{\partial n_e}{\partial U_F}$ and have $\frac{\partial n_e}{\partial U_F} n_e = (1/2) \frac{n_e}{U_F}$ in SMFs. Due to deal with exchange correction under this condition, the SEF of FGP model has some difference to compare with other SES models.

Basing on previous works (Peng et al. (2007); Gao et al. (2013)), which considered the quantum effects in SMFs, by introducing the Dirac δ -function and Pauli exclusion principle, we discuss Dirac equation and the quantization of Landau levels of electrons under the relativistic conditions in SMFs. The results show that the stronger the magnetic field, the higher Fermi energy of electrons in SMFs becomes. According relativistic theory in SMFs, we detailed evaluate the SES problem and ESP by taking into account the quantum effects. The results show that the ESP can increase and gets to the maximum value of 0.1 Mev by SMFs. The SEF also increases greatly and even gets to the maximum value of five by SMFs (e.g. $\rho_7 = 0.01, T_9 = 0.2, B_{12} = 10^3 \text{G}$).

4.2. Investigation of the nuclear reaction rates

It is well known that, in explosive hydrogen burning stellar environments, the nuclear reaction $^{23}\text{Mg}(p, \gamma)^{24}\text{Al}$ plays a key role for breaking out of the Ne-Na cycle to heavy nuclear species (i.e. Mg-Al cycle). Therefore, it is very important for accurate determinate the rates for the reaction $^{23}\text{Mg}(p, \gamma)^{24}\text{Al}$. However, the resonance energy has a large uncertainty due to the inconsistent $^{24}\text{Mg}(^3\text{He}, t)^{24}\text{Al}$ measurements mentioned. And it may lead to a factor of 5 variation in the reaction rate at $T_9 = 0.25$ because of its exponential dependence on E_r (Visser et al. 2007). Therefore, some author discussed in detail the contributions from several important resonance states, such as (Wallace et al. 1981; Wiescher et al. 1986; Kubono et al. 1995; Visser et al. 2007). In order to reduce the uncertainty of the reaction rates in this paper, we reference some information about this reaction and the values of the E_{r_i}, E_x and corresponding to $\omega\gamma_i$ and some average values of $\omega\gamma_i$ are adopted and listed in Table 2. According to these information, we analysis the total rates for these five SES model.

Figure 7 shows the comparison of total resonant rates as a function of T_9 in the case without SES with those of the SES models of Liolios, Dewitt, and LD, FGP, LJ. One can see that different SES models have different effect on the resonant rates. The calculated rates show that our model will be dominant status compared with those of other models at relatively low density (e.g. $\rho_7 = 0.01, 0.1$) and the rates will get to the maximum of 526.3 at $T_9 = 5$. On the contrary, the rates of LD's model will always be the lesser value and the maximum is about 285 at $T_9 = 3.6$. The rates of FGP's model increase with increasing of density and temperature in SMFs and even increase to 507.

The total resonant rates and the rates for four part resonance states as a function of T_9 for different SES model are showed in **Figure 8**. The calculations of $\lambda_{r_{0i}}$ ($i = 1, 2, 3, 4$) and the λ_{r_0} are the rates of four part resonance states and the total resonance rates in the

case without SES and SMFs, respectively. The results show that the contributions of the four resonant to the total reaction rate have obvious difference at the stellar temperatures range of $T_9 = 0.1 \sim 5$. With increasing of temperatures, the rates are very sensitive to the stellar temperatures and increases quickly. One can find that the contribution of resonance state of $E_r = 478\text{keV}$ is dominates to the total reaction rates when $T_9 = 0.2 \sim 1.681$, but the $E_r = 663\text{keV}$ resonance is the most important at high temperatures when $T_9 > 1.681$ and the rates will get to the maximum of 296.4 at $T_9 = 5.186$. On the contrary, the $E_r = 939\text{keV}$ as well as $E_r = 1029\text{keV}$ resonance are negligible compared to the former two lower resonance over the whole temperature range.

The rates of LD's model only have rarely related to density and always are less than the rates λ_{r0} except for $T_9 < 3.307$ in **Figure 8**. Due to SES in SMFs the rates of LD decrease about 20.49% to compare with λ_{r0} . However, the rates of FGP's model increase about 4.38% due to SES in SMFs. As increasing of density, temperature and magnetic field, the growth of the rates will get very slower. However, the rates in our model increase about 4.28% at density of $\rho_7 = 0.001$ due to SES.

The results about the factor C_i ($i = 1, 2, 3$) is plotted in **Figure 9**. One can find that the results of LD's model are in good agreement with those of FGP at relatively low density (e.g. $\rho_7 = 0.01$). With increasing of temperature and magnetic field, the factor of LD's model increases greatly. However, the factor for FGP's model gets to the maximum of 0.5478 at $\rho_7 = 0.1, T_9 = 0.5, B_{12} = 60.76$. The factor of our model also increases greatly with increasing of the magnetic field and gets to the maximum of 0.9 at $\rho_7 = 0.01, T_9 = 0.5, B_{12} = 1000$.

Table 3 and 4 give a brief description of the factor S_i ($i = 1, 2, 3$) for LD's, FGP's, and LJ's models when $B_{12} = 10, 10^3$, respectively. With increasing of density and temperature, the results of LD's model are in good agreement with those of FGP, but disagreement with

our results at $B_{12} = 10$. This is because that the electron Fermi energy of our model is lower than those of LD and FGP in relatively low magnetic field environment. However, when the magnetic field increases from $B_{12} = 10$ to 10^3 , factor S_3 increases about 2 ~ 3 orders magnitude (i.e. from 0.1749 to 25.5680 and from 0.0022 to 3.8848) when $\rho_7 = 0.01, T_9 = 0.1$ and $\rho_7 = 0.1, T_9 = 0.2$, respectively. When $B_{12} = 10^3$ factor S_3 (our model) is about 39.74, 5.69, 1.56 times larger than S_2 (FGP's model) at $\rho_7 = 0.03, T_9 = 0.2$, $\rho_7 = 0.05, T_9 = 0.2$ and $\rho_7 = 0.1, T_9 = 0.2$, respectively. From what has been discussed above, we find the LD's model is only adapted to the relatively low magnetic field and low density surroundings. Furthermore, the FGP's and LD's model are both unadapted to relatively low density, and high magnetic field surroundings (e.g. $\rho_7 < 0.1, B_{12} > 10^2$). However, our model can be well adapted to relatively high magnetic field and low density surroundings (e.g. $B_{12} > 10^2, \rho_7 < 0.05$) in the crust of magnetar.

Our calculated rates are compared with those of LD and FGP by the factor q_j ($j = 1, 2$) in **Figure 10**. We find that our results are in good agreement with those of LD and FGP at relatively low density (i.e. $\rho_7 = 0.01$) for $B_{12} = 10 \sim 10^2$. However, the rates of our model can be 1.58 times larger than those of FGP for $B_{12} = 10^3, \rho_7 = 0.01, T_9 = 0.2$. And can be around three orders of magnitude larger than those of LD for $B_{12} = 10^3, \rho_7 = 10, T_9 = 1$.

Summing up the above discussion, our work differs from earlier works (LD and FGP) in that we derive new results for the SES theory in an SMFs and the rates for nuclear reaction, which we use in the SES theory calculations in relativistic strongly magnetic field surrounding basing on the the Dirac δ -function and Pauli exclusion principle. We also make detailed comparison among the results for the nuclear reaction rates of different SES model in SMFs. We correct the traditional popular viewpoint about the Fermi energy in SMFs (i.e. $U_F \propto 2.67B_{12}^{-2}k(Y_e\rho)^2$), which have been derived by Canuto et al. (1968, 1971), Lai et al. (1991); Lai (2001), and Fushiki et al. (1989). Their opinion shows that the stronger the

magnetic fields, the lower the electron Fermi energy becomes. The main problems we investigate are how magnetic fields affect the electron Fermi energy and electron screening potential that enters the theory of nuclear reaction rates. We show that this effect can increase nuclear reaction rates of $^{23}\text{Mg} (p, \gamma)^{24}\text{Al}$ by several orders magnitude. A more precise thermonuclear rates of $^{23}\text{Mg} (p, \gamma)^{24}\text{Al}$ will help us to constrain the determination of nuclear flow out of the Ne-Na cycle, and production of $A \geq 20$ nuclides, in explosive hydrogen burning over a temperature range $0.2 \leq T \leq 1.0$ GK.

As everyone knows, the progenitor double neutron star systems have long been known to exist (Hulse et al. 1975). The merging of two neutron stars (NS-NS) or black hole and neutron star (BH-NS) that make up a binary system is of interest both because it is a powerful source of gravitational waves and because it might be the central engine of gamma-ray bursts. Paczynski (1986) and Eichler et al. (1989) first discussed the binary compact object model for merging neutron stars, which is regarded as possible sources of gamma ray burst. The merger of a neutron star with a black hole also investigated by Paczynski (1991) and Narayan et al. (1992). Some works about hydrodynamical numerical simulation of the merging of NS-NS or BH-NS also have been carried out by Ruffert et al. (1998); Bauswein et al. (2014); Kiuchi et al. (2014). Their researches show that the problem on nucleosynthesis is a very interesting and challenging issue. In the process of merger, a good deal of heavy elements (e.g. ^{26}Al), produced from the nucleosynthesis process, may be thrown out to interstellar space. Therefore, our results may help us understand why some elements (e.g. ^{26}Al) is overabundance and our works may have important significance to the future investigations of the change of element abound of interstellar space and evolution of magnetars.

5. Conclusions

Basing on the relativistic theory in SMFs, we investigate the problem of SES, and the influence on the nuclear reaction of $^{23}\text{Mg} (p, \gamma)^{24}\text{Al}$ by LD's, FGP's, and LJ's strong screening models in SMFs. We also analyse the Landau energy level and the electron Fermi energy in details due to the effects of SMFs. The results show that the effects of SES on the thermonuclear reaction rates are remarkable in SMFs. The rates can be increased by around three orders of magnitude. And the rates of our model are in good agreement with those of LD and FGP at relatively low density and magnetic fields (e.g. $\rho_7 < 0.01$) for $B_{12} < 10^2$. In relatively low magnetic fields (e.g. $B_{12} < 1$), the SES of LD's and FGP's model has strong influence on the rates of nuclear reaction to compare to our model. However, the rates of our model can be about 1.58 times and three orders magnitude higher than those of FGP and LD in relatively high magnetic fields and low density surroundings (e.g. $B_{12} \geq 10^2$, $\rho_7 < 0.05$), respectively.

On the other hand, one can conclude that our calculated rates increase greatly and even exceed by three orders magnitude at the same density and temperature with increasing of SMFs. For example, when B_{12} increases from 10 to 10^3 , the rates increase from 0.1749 to 25.5680 at $\rho_7 = 0.01, T_9 = 0.1$, and from 0.0022 to 3.8848 at $\rho_7 = 0.1, T_9 = 0.2$. The considerable increase of the reaction rates for $^{23}\text{Mg} (p, \gamma)^{24}\text{Al}$ implies that more ^{23}Mg will escape the Ne-Na cycle due to SES in SMFs. Then it will make the next reaction convert more $^{24}\text{Al} (\beta^+, \nu)^{24}\text{Mg}$ to participate in the Mg-Al cycle. It may lead to synthesize a large amount of heavy elements (e.g. ^{26}Al) at the crust of magnetars. These heavy elements (e.g. ^{26}Al), which are produce from the nucleosynthesis process, may be thrown out due to the compact binary mergers of double neutron star (NS-NS) or black hole and neutron star (BH and NS) systems. Thereby the results, we derived may help to understand why the ^{26}Al is always overabundance in the interstellar space. However, the problem of the overabundance

of ^{26}Al in interstellar matter needs much more efforts to consider the influence by many factors (such as the resonant energy, nuclear reaction pathway, element abundance, the density, and the temperature, as well as the strength of magnetic fields). These problems will be our next issues to discuss.

In summary, we describe our analytical results about the SES theory in SMFs and obtain some information of the screened rates by calculating the SEF on the surface of magnetars. It may improve our understanding of the thermal evolution and thermal spectrum of magnetars. However, the problem about the effects of SES in SMFs on the nuclear reaction is always a challenging topic, which is interesting to many astrophysicists due to the fact that the SEF is related to the ESP, density, temperature and strength of magnetic fields in different SES model and surroundings. These discrepancies may produce important and profound influence on the nuclear reaction pathway, nucleosynthesis for some heavy nuclei, and the energy generation rate, as well as the element abundance on the surface of magnetars. Hence, our research may become a good foundation for the future investigation of the evolution and numerical simulation of magnetars, and may be important significance to future research on nuclear astrophysics.

This work was supported by the National Basic Research Program of China (973 Program) under grant 2014CB845800, the National Natural Science Foundation of China under grants 11222328, 11333004, 11363003, and the Natural Science Foundation of Hainan province under grant 114012.

REFERENCES

- Ashcroft, N. W., & Mermin, N. D., 1976, *Solid State Physics* (Saunders College: Philadelphia)
- Audi, G., & Wapstra, A. H., 1995, *Nucl. Phys. A.*, 595, 409
- Bahcall, J. N., Brown, L., Gruzinov, A., & Sawyer, R., 2002, *A&A*, 383, 291
- Bauswein, A., Ardevol Pulpillo, R., Janka, H.-T., & Goriely, S., 2014, *ApJ*, 795, L9
- Canuto, V., & Chiu, H. Y., 1968, *Phys. Rev.*, 173, 1210
- Canuto, V., & Chiu, H. Y., 1971, *Space. Sci. Rev.*, 12, 3
- Dewitt, H. E., 1976, *Phys. Rev. A.*, 14, 1290
- Das, Upasana., & Mukhopadhyay, Banibrata., 2012, *Phys. Rev. D.*, 86, 2001
- Eichler, D., Livio, M., Piran, T., & Schramm, D. N., 1989, *Nature*, 340, 126
- Endt, P. M., 1998, *Nucl. Phys. A.*, 633, 1
- Fowler, W. A., Caughlan, G. R., & Zimmerman, B. A., 1967, *ARA&A.*, 5, 525
- Fushiki, I., Gudmundsson, E. H., & Pethick, C. J., 1989, *ApJ*, 342, 958
- Gao, Z. F., Peng, Q. H., Wang, N., & Yuan, J. P., 2012, *ApS &S*, 342, 55
- Gao, Z. F., Wang, N., Peng, Q. H., Li, X. D., & Du, Y. J., 2013, *MPLA.*, 28, 1350138
- Graboske, H. C., & DeWitt, H. E., 1973, *ApJ*, 181, 457
- Herndl, H., Fantini, M., Iliadis, C., Endt, P. M., & Oberhummer, H., 1998, *Phys. Rev. C.*, 58, 1798

- Hulse, R. A., & Taylor, J. H. 1975, *ApJ*, 201, L55
- Iliadis, C., D’Auria, J. M., Starrfield, S., et al., 2001, *ApJS*, 134, 151
- Kadomtsev, B. B., 1970, *Zh. Eksp. Teor. Fiz.* 58, 1765
- Kiuchi, K., Kyutoku, K., Sekiguchi, Y., Shibata, M., & Wada, T., 2014, *Phys. Rev. D.*,90, 041502
- Kubo, R., 1965, *Statistics Mechanics*, (Amsterdam: North-Holland Publishing Co.), pp. 278, 280
- Kubono, S., Kajino, T., & Kato, S., 1995, *Nucl. Phys. A.*, 588, 521
- Kravchuk, P. A., & Yakovlev, D. G., 2014, *Phys. Rev. C.*, 89, 015802
- Landau, L. D., & Lifshitz, E. M., 1977, *Quantum mechanics*, (3rd ed., Oxford: Pergamon Press), p.457
- Lai, D., & Shapiro, Stuart. L., 1991, *ApJ*, 383, 745
- Lai, D., 2001, *Rev. Mod. Phys.*, 73, 629
- Lane, A. M., & Thomas, R. G., 1958, *Rev. Mod. Phys.*, 73, 629
- Lattimer, J. M., Pethick, C. J., Ravenhall, D. G., & Lamb, D. Q., 1985, *Nucl. Phys. A.*, 432, 646
- Liu, J. J., 2013, *MNRAS*, 433, 1108
- Liu, J. J., 2014, *MNRAS*, 438, 930
- Liolios, T. E., 2000, *EPJA.*, 9, 287
- Liolios, T. E., 2001, *Phys. Rev. C.*, 64, 018801

- Lotay, G., Wood, P. J., Seweryniak, D., et al., 2008, *Phys. Rev. C.*, 77, 2802
- Narayan, R., Paczynski, B., & Piran, T., 1992, *ApJ*, 395, L83
- Paczynski, B., 1986, *ApJ*, 308, L43
- Paczynski, B., 1991, *Acta Astron.*, 41, 257
- Pathria, R. K., 2003, *Statistics Mechanics*, 2nd., (Singapore: Isevier.), pp. 280
- Peng, Q. H., & Tong, H., 2007, *MNRAS*, 378, 159
- Ruffert, M., & Janka, H.-Th., 1998, *A&A*, 338, 535
- Salpeter, E. E., & van Horn, H. M., 1969, *ApJ*, 155, 183
- Salpeter, E. E., 1954, *AuJPh.*, 7, 373
- Schatz, H., Aprahamian, A., Goerres, J. et al., 1998, *Phys. Rep.*, 294, 167
- Stolzmann, W., & Bloecker, T., 1996, *A&A*, 314, 1024
- Visser, D. W., Wrede, C., Caggiano, J. A., et al., 2007, *Phys. Rev. C.*, 76, 065803
- Wallace, R. K., & Woosley, S. E., 1981, *ApJS.*, 45, 389.
- Wiescher, M., Gorres, J., Thielemann, F.-K., & Ritter, H., 1986, *A&A*, 160, 56
- Yakovlev, D. G., & Shalybkov, D. A., 1989, *Astrophys. Space. Phys. Rev.*, 7, 311

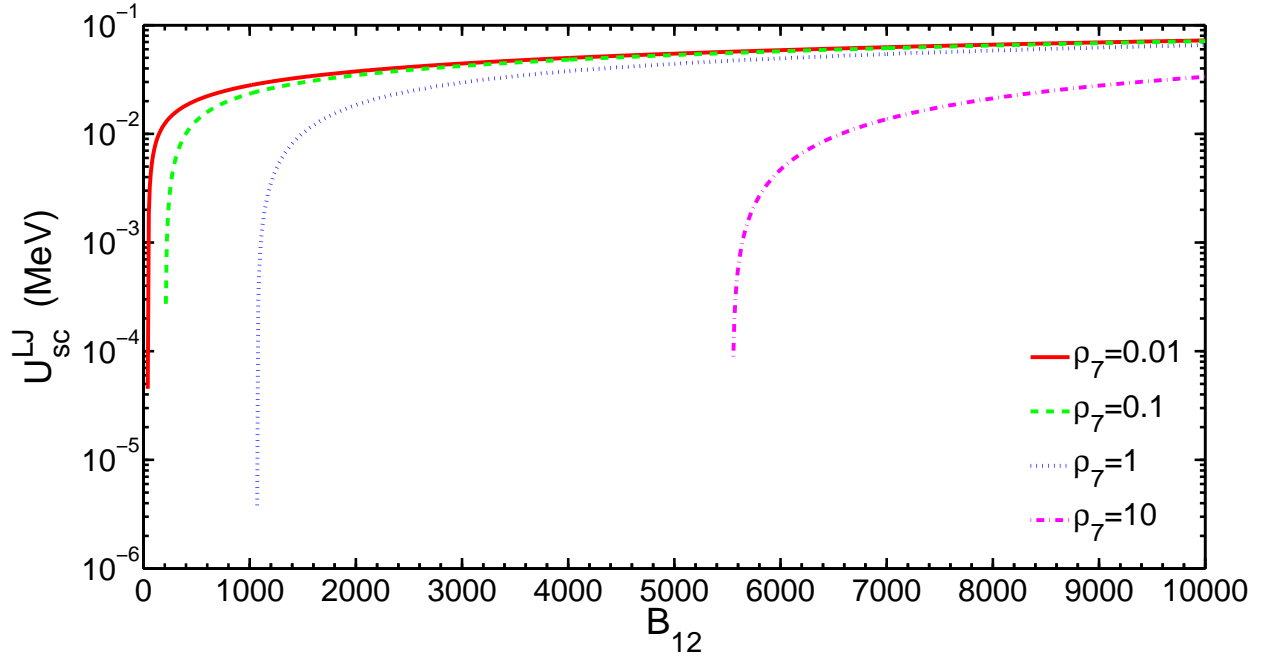


Fig. 1.— The electron screening potential as a function of B_{12} of LJ’s model for some typical astronomical condition.

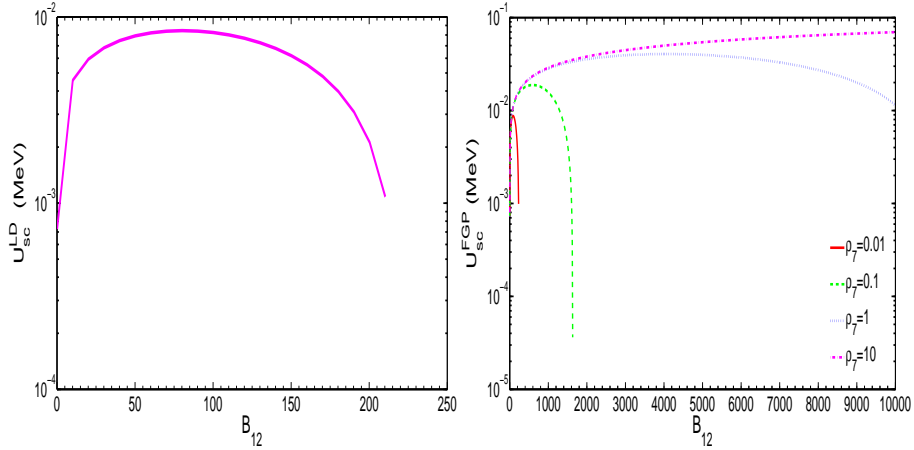


Fig. 2.— The electron screening potential as a function of B_{12} of LD’s, and FGP’s model for some typical astronomical condition.

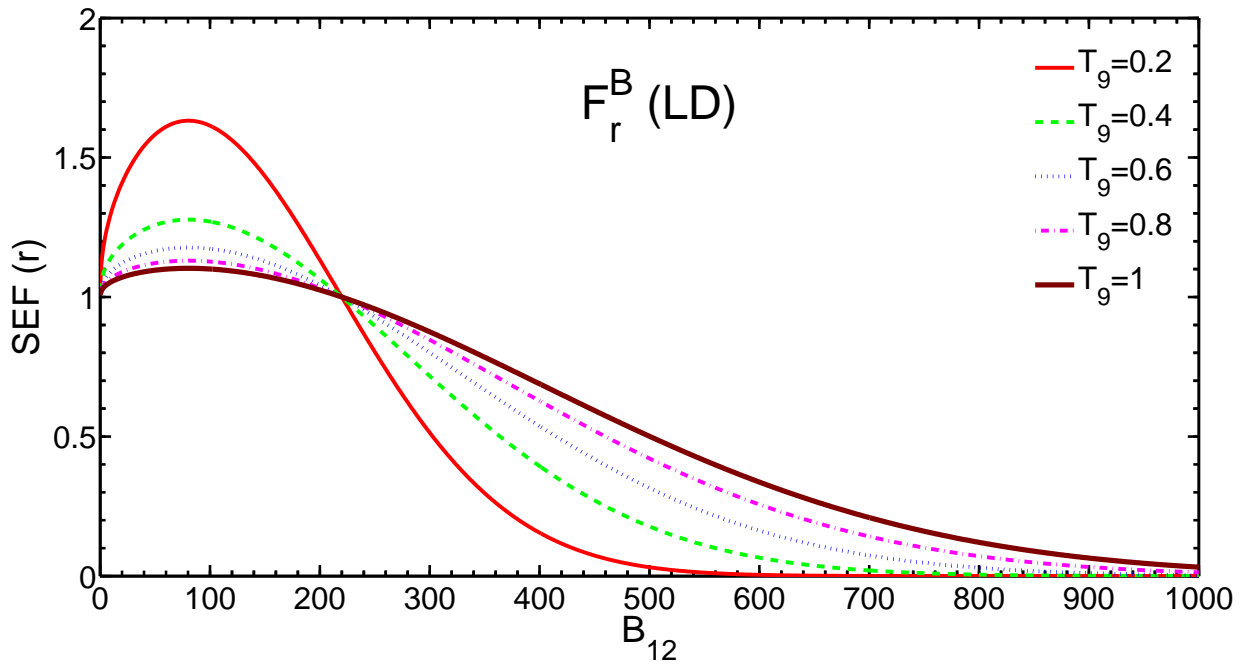


Fig. 3.— The resonant SEF for the model of LD as a function of B_{12} in the case with SES and SMFs.

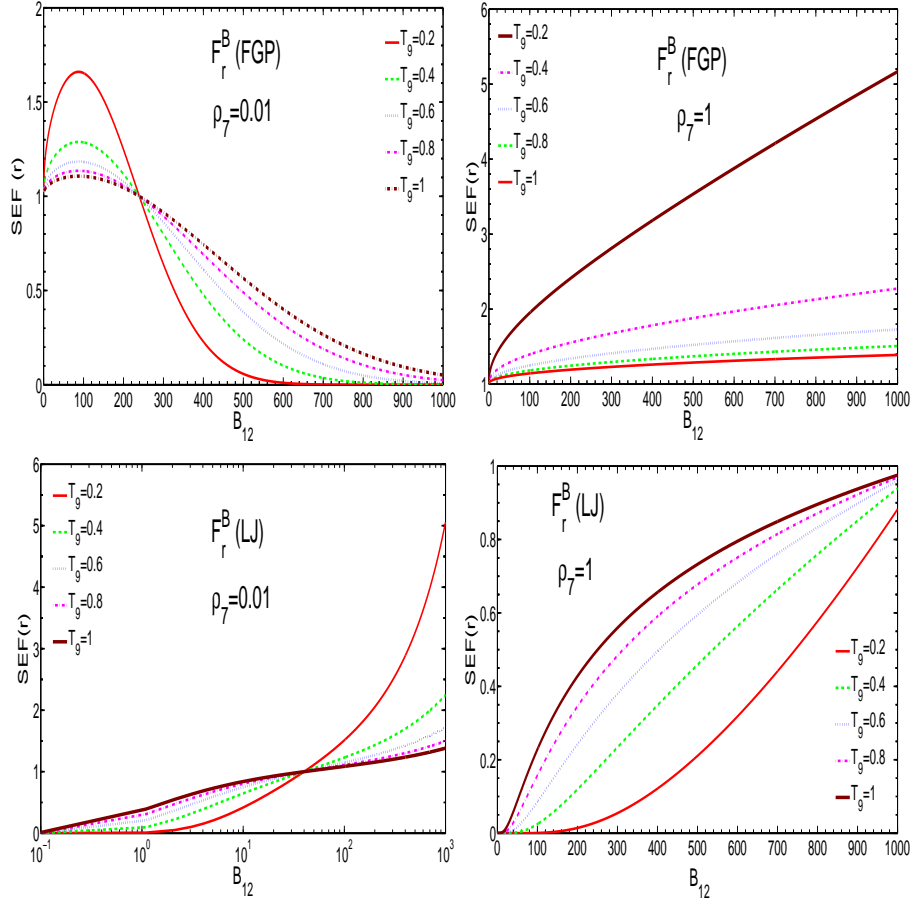


Fig. 4.— The resonant SEF for the model of FGP and LJ as a function of B_{12} in the case with SES and SMFs.

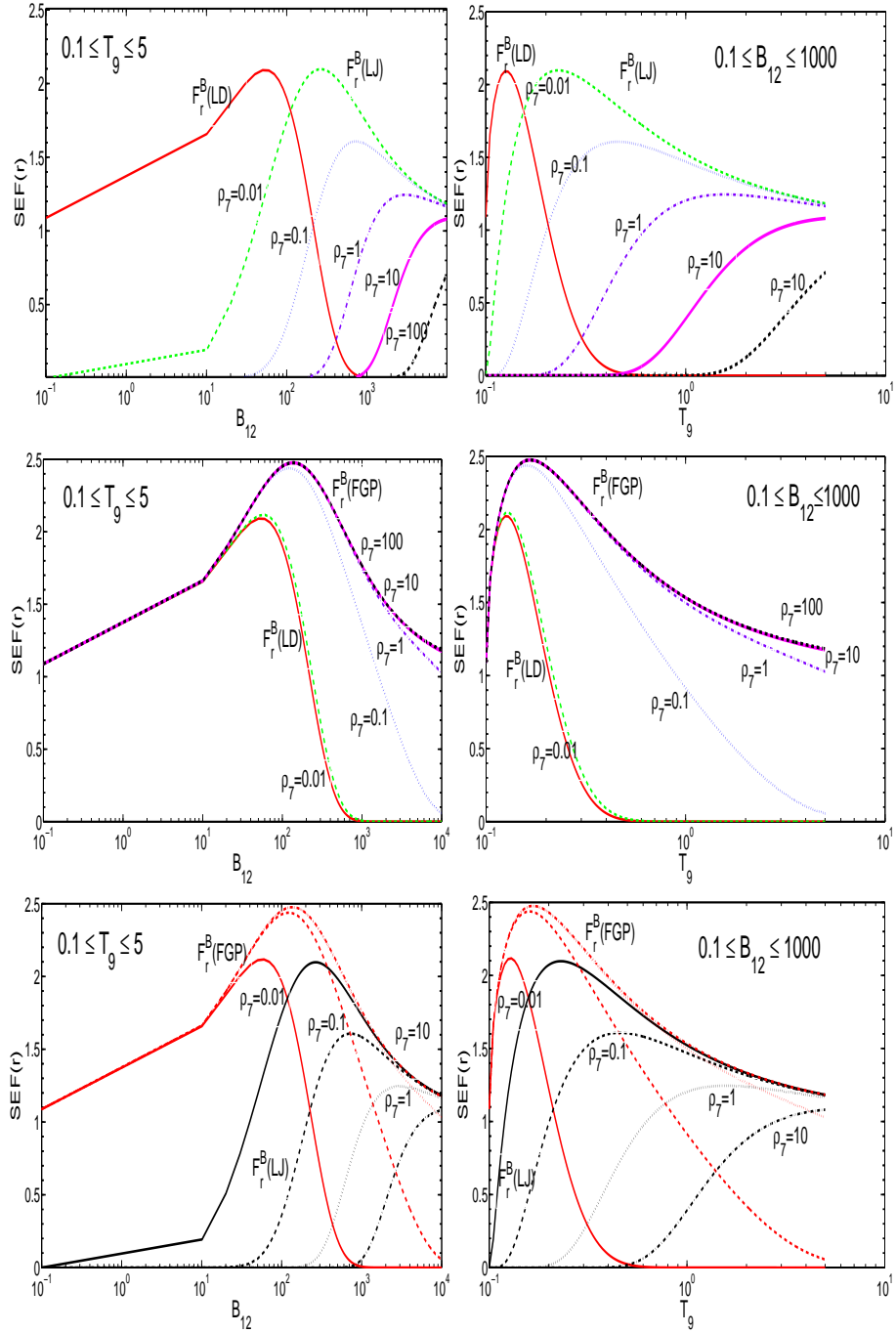


Fig. 5.— The comparisons are plotted for some typical astronomical condition of the resonant SEF among the three models of LJ, LD, and FGP in the case with SES and SMFs.

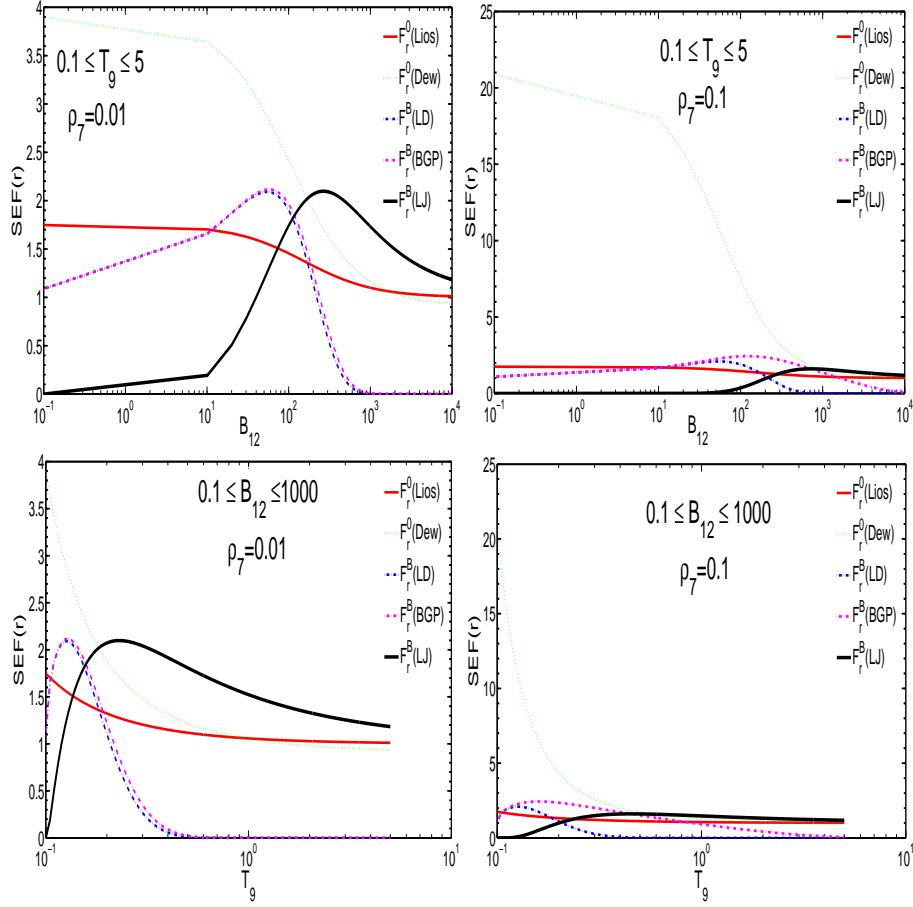


Fig. 6.— The comparisons of the resonant SEF for the model of Liolios, Dewitt with those of models of LD, FGP, and LJ.

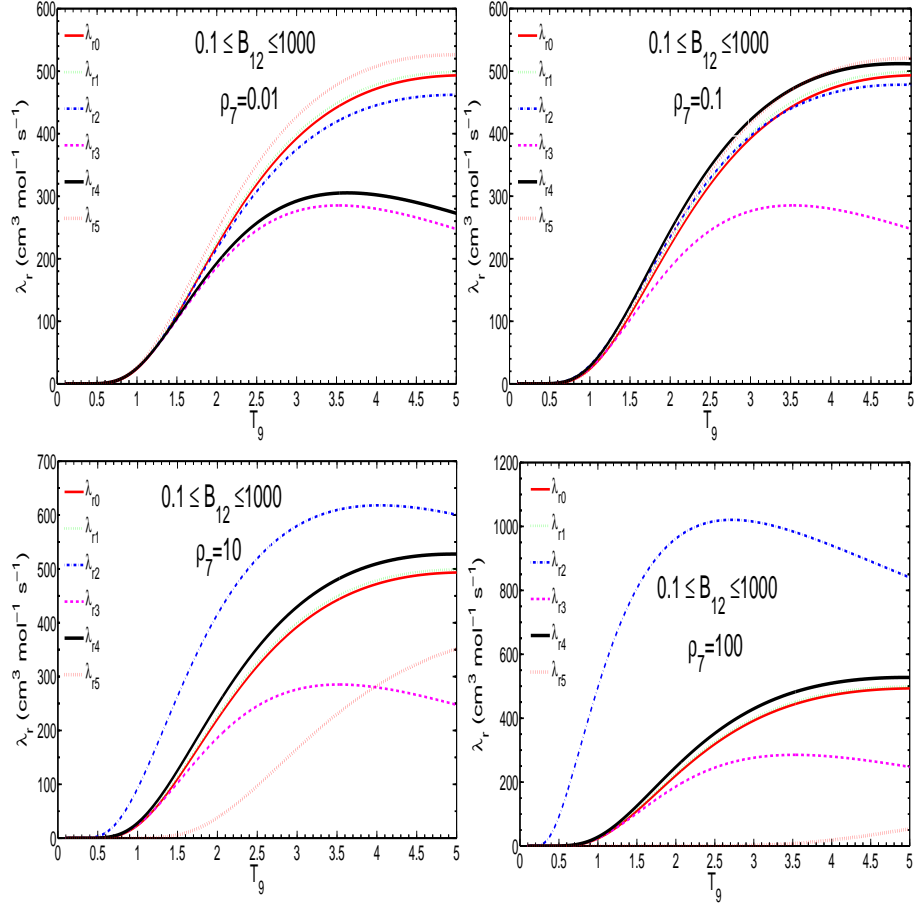


Fig. 7.— The comparison of total resonant rates as a function of T_g for some typical astronomical condition in the case without SES with those of the SES models of Liolios, Dewitt and the models of LD, FGP, and LJ.

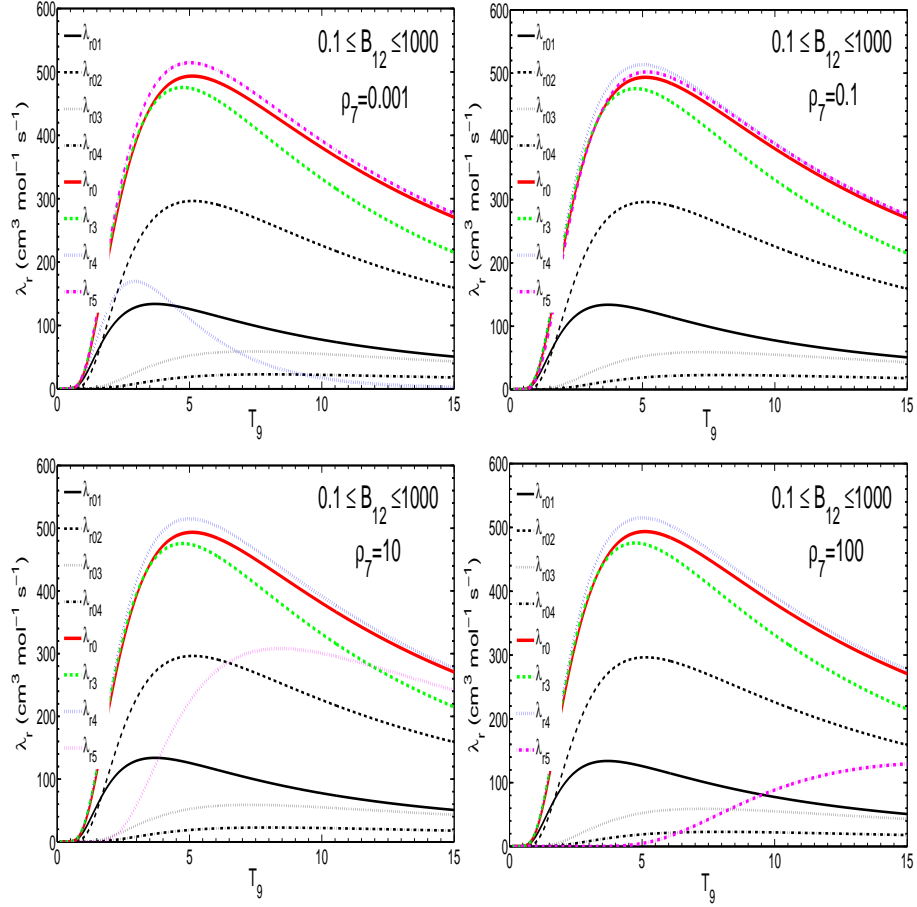


Fig. 8.— The comparison of total resonant rates and the rates for four part states as a function of T_9 in the case without SES with those of the SES models of LD, FGP, and LJ.

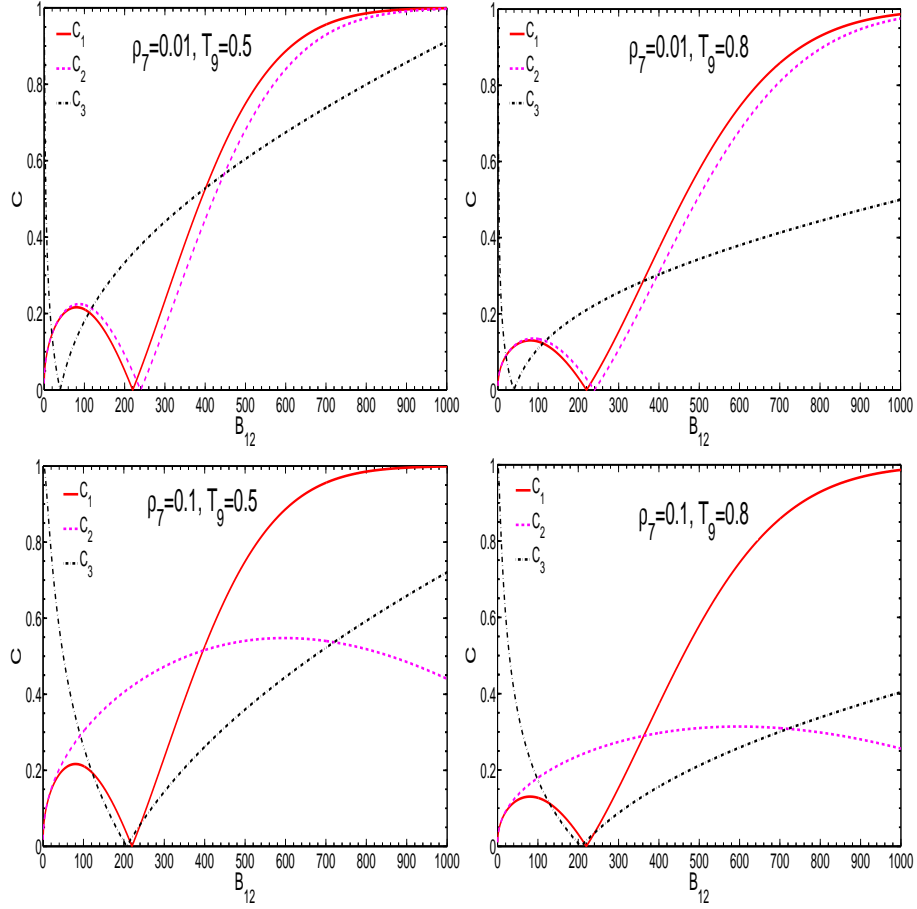


Fig. 9.— The error factor C_i , ($i = 1, 2, 3$) as a function of B_{12} for some typical astronomical condition.

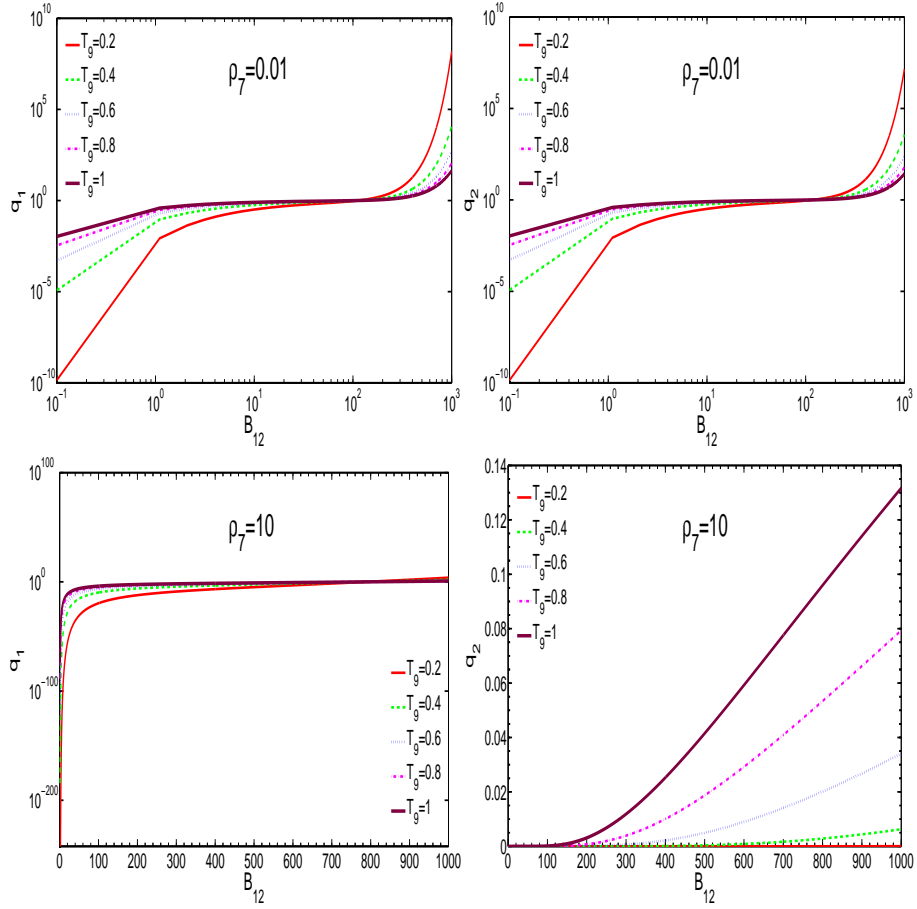


Fig. 10.— The scale factor q_j , ($j = 1, 2$) as a function of B_{10} for some typical astronomical condition.

Table 1. The comparisons for some typical astronomical condition of the resonant SEF in the case without SES for the model of Dewitt, Liolios with those of model of LD, FGP, and LJ in the case with SES and SMFs

ρ_7	T_9	$B_{12} = 10$					$B_{12} = 10^3$		
		$F_r^0(\text{Lios})$	$F_r^0(\text{Dew})$	$F_r^B(\text{LD})$	$F_r^B(\text{FGP})$	$F_r^B(\text{LJ})$	$F_r^B(\text{LD})$	$F_r^B(\text{FGP})$	$F_r^B(\text{LJ})$
0.01	0.1	1.7475	3.8973	1.6956	1.6964	0.1749	1.0725e-15	1.3472e-13	25.5680
0.05	0.1	1.7475	10.9451	1.6956	1.7013	8.4513e-4	1.0725e-15	0.6045	19.5717
0.1	0.2	1.3219	4.3605	1.3021	1.3045	0.0022	3.2750e-8	2.4894	3.8848
0.1	0.3	1.2051	2.5873	1.1922	1.1941	0.0174	1.0221e-5	1.8371	2.4713
0.2	0.3	1.2045	3.3934	1.1924	1.1939	9.1604e-4	1.0236e-5	2.4990	2.1361
0.3	0.4	1.1497	2.8170	1.1411	1.1422	7.7822e-4	1.8097e-4	2.1178	1.6055
1.0	0.5	1.1181	3.5124	1.1113	1.1122	6.2630e-7	0.0011	1.9290	0.9512
10	0.7	1.0830	7.2692	1.0780	1.0791	6.2012e-9	0.0072	1.6142	0.0894

Table 2. Resonance parameters for the reaction $^{23}\text{Mg} (p, \gamma) ^{24}\text{Al}$

E_x (MeV) ^a	E_x (MeV) ^b	J^π	E_{r_i} (MeV) ^c	Γ_p	Γ_γ	$\omega\gamma_i$ (meV) ^d	$\omega\gamma_i$ (meV) ^e	$\omega\gamma_i$ (meV) ^f
2.349±0.020	2.346±0.000	3 ⁺	0.478	185	33	25	27	26
2.534±0.013	2.524±0.002	4 ⁺	0.663	2.5e3	53	58	130	94
2.810±0.020	2.792±0.004	2 ⁺	0.939	9.5e5	83	52	11	31.5
2.900±0.020	2.874±0.002	3 ⁺	1.029	3.4e4	14	12	16	14

Note. — ^a is adopted from Ref. (Endt 1998); ^b from Ref.(Visser et al. 2007); ^c from Ref.(Audi et al. 1995); ^d from Ref.(Herndl et al. 1998) and ^e from Ref.(Wiescher et al. 1986), ^fis adopted in this paper.

Table 3: Comparisons of the rates of λ_r^0 , which are in the case without SES and SMFs with those of the LD ($\lambda_r^{\text{scB}}(\text{LD})$), FGP ($\lambda_r^{\text{scB}}(\text{FGP})$) and our calculations $\lambda_r^{\text{scB}}(\text{LJ})$ in the case with SES for some typical astronomical conditions at $B_{12} = 10$, respectively. The S_i is noted $S_i = \lambda_{ri}^{\text{scB}}/\lambda_r^0$, $i = 1, 2, 3$ is the rates of LD's, FGP's, and LJ's model, respectively.

ρ_7	T_9	λ_r^0	$B_{12} = 10$			S_1	S_2	S_3
			$\lambda_r^{\text{scB}}(\text{LD})$	$\lambda_r^{\text{scB}}(\text{FGP})$	$\lambda_r^{\text{scB}}(\text{LJ})$			
0.01	0.1	1.0942e-19	1.8552e-19	1.8561e-19	1.9138e-20	1.6956	1.6964	0.1749
0.02	0.1	1.0942e-19	1.8552e-19	1.8598e-19	4.0569e-21	1.6956	1.6998	0.0371
0.03	0.1	1.0942e-19	1.8552e-19	1.8608e-19	1.0413e-21	1.6956	1.7007	0.0095
0.03	0.2	4.2967e-8	5.5949e-8	5.6034e-8	4.1916e-9	1.3021	1.3041	0.0976
0.04	0.2	4.2967e-8	5.5949e-8	5.6041e-8	2.2448e-9	1.3021	1.3043	0.0522
0.05	0.2	4.2967e-8	5.5949e-8	5.6044e-8	1.2491e-9	1.3021	1.3043	0.0291
0.1	0.2	4.2967e-8	5.5949e-8	5.6051e-8	9.3383e-11	1.3021	1.3045	0.0022
0.2	0.4	0.0163	0.0186	0.0186	8.5713e-5	1.1411	1.1422	0.0053
0.3	0.5	0.1925	0.2140	0.2141	6.2713e-4	1.1114	1.1122	0.0033
0.5	0.6	0.9764	1.0663	1.0669	8.5404e-4	1.0920	1.0927	8.7465e-4
0.7	0.8	7.2550	7.7500	7.7537	0.0079	1.0682	1.0687	0.0011
1.0	0.9	14.0604	14.9100	14.9162	0.0050	1.0604	1.0609	3.5785e-4

Table 4: Comparisons of the rates of λ_r^0 , which are in the case without SES and SMFs with those of the LD ($\lambda_r^{\text{scB}}(\text{LD})$), FGP ($\lambda_r^{\text{scB}}(\text{FGP})$) and our calculations $\lambda_r^{\text{scB}}(\text{LJ})$ in the case with SES for some typical astronomical conditions at $B_{12} = 10^3$, respectively. The S_i is the same as in Table 3.

ρ_7	T_9	λ_r^0	$B_{12} = 10^3$			S_1	S_2	S_3
			$\lambda_r^{\text{scB}}(\text{LD})$	$\lambda_r^{\text{scB}}(\text{FGP})$	$\lambda_r^{\text{scB}}(\text{LJ})$			
0.01	0.1	1.0942e-19	1.1735e-34	1.4740e-32	2.7975e-18	1.0725e-15	1.3472e-13	25.5680
0.02	0.1	1.0942e-19	1.1735e-34	6.4612e-24	2.5883e-18	1.0725e-15	5.9052e-5	23.6555
0.03	0.1	1.0942e-19	1.1735e-34	1.5306e-21	2.4177e-18	1.0725e-15	0.0140	22.0969
0.03	0.2	4.2967e-8	1.4072e-15	5.0819e-9	2.0198e-7	3.2750e-8	0.1183	4.7007
0.04	0.2	4.2967e-8	1.4072e-15	1.7120e-8	1.9575e-7	3.2750e-8	0.3984	4.5559
0.05	0.2	4.2967e-8	1.4072e-15	3.3408e-8	1.9009e-7	3.2750e-8	0.7775	4.4240
0.1	0.2	4.2967e-8	1.4072e-15	1.0696e-7	1.6692e-7	3.2750e-8	2.4894	3.8848
0.2	0.4	0.0163	2.9459e-6	0.0324	0.0288	1.8097e-4	1.9876	1.7669
0.3	0.5	0.1925	1.9523e-4	0.3509	0.2812	0.0010	1.8227	1.4604
0.5	0.6	0.9764	0.0031	1.6579	1.1949	0.0032	1.6979	1.2237
0.7	0.8	7.2550	0.0976	10.8789	7.8159	0.0135	1.4995	1.0773
1.0	0.9	14.0604	0.3053	20.2526	13.6742	0.0217	1.4404	0.9725